Treatment of Focal Muscle Stiffness with Hyaluronidase Injections

13

Preeti Raghavan, Alexandra Gordon, Ryan Roemmich, and Antonio Stecco

…the beauty and strength of the mechanical construction lie not in one part or in another, but in the harmonious concatenation which all the parts, soft and hard, rigid and flexible, tension bearing and pressure bearing, make up together.

—D'Arcy Thompson, On Growth and Form, 1917.

- Spasticity develops because of injury to the central nervous system. However, secondary changes within the connective tissue of the muscle also contribute to muscle stiffness.
- The hyaluronan hypothesis postulates that the accumulation and biophysical alteration of hyaluronan, a high molecular weight glycosaminoglycan that normally acts as a lubricant within the extracellular matrix of muscles, promotes the development of muscle stiffness and progression to fibrosis and muscle contracture.

The original version of this chapter was revised. Affiliation of Alexandra Gordon has been updated. The correction to this chapter can be found at https://doi.org/10.1007/978-3-030-96900-4_15

P. Raghavan
Departments of Physical Medicine and Rehabilitation and Neurology, The Johns Hopkins University School of Medicine, Baltimore, MD, USA
e-mail: praghavan@jhmi.edu

A. Gordon
Albert Einstein College of Medicine, Bronx, NY, USA
e-mail: alexandra.gordon@einsteinmed.edu

R. Roemmich
Department of Physical Medicine and Rehabilitation, Johns Hopkins University School of Medicine, Baltimore, MD, USA
e-mail: rroemmi1@jhu.edu

A. Stecco (✉)
Rusk Rehabilitation, NYU Grossman School of Medicine, New York, NY, USA
e-mail: Antonio.stecco@nyulangone.org

P. Raghavan (ed.), *Spasticity and Muscle Stiffness*,
https://doi.org/10.1007/978-3-030-96900-4_13

- Intramuscular injections of the enzyme hyaluronidase, which catabolizes the altered hyaluronan polymer, were shown to reduce muscle stiffness and increase passive and active range of motion in patients with spasticity.
- This chapter discusses the preliminary evidence for the emerging treatment of muscle stiffness using the enzyme hyaluronidase and its potential to prevent fibrosis and contracture.

Introduction

Hyaluronidases are a group of enzymes distributed throughout the animal kingdom that regulate the metabolism of hyaluronic acid (hyaluronan, HA). The hyaluronan hypothesis of muscle stiffness postulates that the accumulation and biophysical alteration of HA in the extracellular matrix (ECM) of muscle leads to the development of muscle stiffness [1, 2]. Chapter 6 describes the evidence for the role of altered HA metabolism in the development of increased passive resistance to movement. HA is a non-sulfated high molecular weight glycosaminoglycan (GAG) and a major component of the endomysium, perimysium, and epimysium which together constitute the ECM of the muscle [3]. In the healthy state, HA in the ECM acts as a lubricant to facilitate sliding and myofascial force transmission within and between muscles [4, 5]. However, disruption in the homeostasis of HA due to reduced clearance and/or increased production, for example, because of paresis and immobility [6] as well as muscle overactivity and compensatory overuse [7, 8], can lead to the accumulation of HA and an alteration in its physiological properties leading to muscle stiffness and increased resistance during passive movement [9, 10] (Fig. 13.1).

GAGs and specifically HA, the largest GAG, can self-organize into diverse supramolecular complexes that determine the physical properties of the tissue [11]. Figure 13.2 shows the various ways in which GAGs can self-organize and form

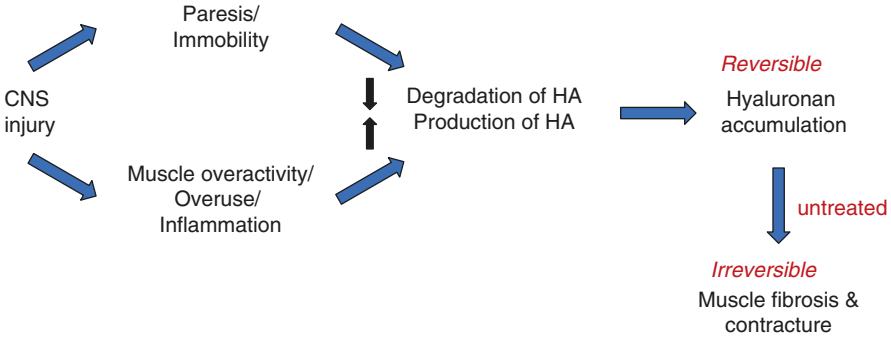

Fig. 13.1 Paresis and immobility after CNS injury can lead to reduced degradation of hyaluronan (HA), whereas muscle overactivity, overuse of compensating muscles, and/or inflammation can lead to increased production of HA. If HA accumulation is untreated, it may contribute to irreversible muscle fibrosis and contracture

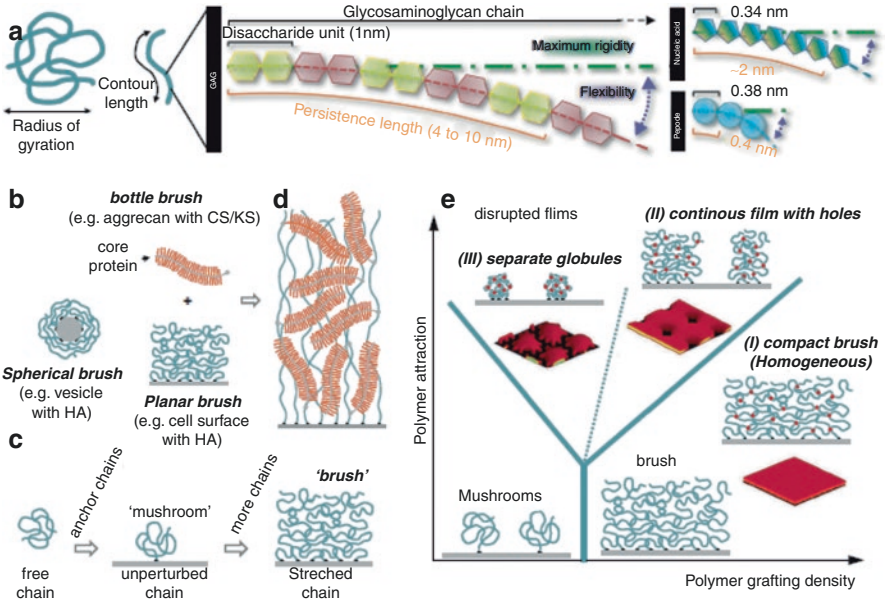

Fig. 13.2 Schematic diagrams illustrating the self-organization of glycosaminoglycans (GAGs), and specifically hyaluronan (HA), from a soft matter physics perspective. (**a**) The radius of gyration and the contour length of polymer chains, and the sizes of the building blocks and persistence lengths for GAGs relative to nucleic acids and (poly)peptides. (**b**) Polymer brushes: a bottle brush forms upon anchorage of chondroitin sulfate (CS) and keratan sulfate (KS) at high density to a core protein (e.g., aggrecan); HA, when retained via attachment to hyaluronan synthases (HASs), can form a planar brush on the cell surface, spherical brushes around extracellular vesicles and cylindrical brushes around cell membrane protrusions. (**c**) Brushes form when the flexible GAG chains are anchored at high density to a substrate. (**d**) Assemblies of GAGs and GAG-rich proteoglycans are intrinsically mechanically soft and swollen owing to the mutual repulsion of GAGs and the high negative charge, providing an osmotic swelling pressure due to associated counter ions. The schematic shows how aggrecan swells and extends HA brushes. (**e**) Crosslinking of GAGs with proteins causes compaction, phase separation, and rigidification. As the attraction between polymers increases (in the case of GAGs by crosslinking with proteins), the film becomes more compact and rigid, and a homogeneous brush (I) can phase separate into heterogeneous films of distinct morphology: a continuous film with holes (II) or separate globules (III). Boundaries between phases are drawn qualitatively and three-dimensional views (red) illustrate the gross morphology of phases I, II, and III. (Modified from Richter RP (2018), with permission)

rigid structures. The aggregation and self-organization of HA polymers is highly dependent on HA concentration, temperature, and pH, which together affect the viscoelasticity of the ECM [5, 12, 13]. The compliant nature of the HA aggregations may explain how physical modalities, such as the application of heat and cold, and physical manipulation, such as stretching and massage, affect the resistance to passive movement in individuals with muscle stiffness with or without spasticity [14, 15]. For example, it has been shown that passive resistance to stretching at slow speeds, which is thought to reflect non-neural muscle stiffness, is increased with the application of a cold stimulus, whereas it is decreased with the application of a

warm stimulus in individuals with spasticity [16]. Repetitive static stretching can lead to a temporary reduction in viscoelastic stress relaxation in individuals with and without spasticity [17, 18]. Increased GAG content is seen in non-spastic myofascial pain and muscle stiffness [19, 20], and deep friction massage has been shown to reduce GAG content as measured by muscle imaging [8]. Taken together, these studies suggest that the alteration in the biophysical properties of HA can affect muscle stiffness. Since hyaluronidases catabolize HA, they could play a critical role in the clearance of HA, particularly in individuals with severe muscle stiffness.

The potential role of HA and hyaluronidase in spasticity may be surmised from a study that demonstrated the presence of HA in the capsular space of the cat muscle spindle, which was responsible for the transcapsular potential across the sensory terminal membrane that makes the sensory nerve ending sensitive to mechanical stimuli. The diffusion of hyaluronidase into the capsular space reduced both resting and stretch-induced impulses in the muscle spindle [21]. HA is also abundant around the nerve endings in the perimysium (see Chap. 6, Fig. 6.9). Excessive amounts of HA in the muscle spindle and around the nerves in the perimysium may affect the stretch reflex response. Furthermore, HA is also a key component of perineuronal nets (PNNs), which refer to the ECM around neurons in the central nervous system (CNS) and are shown to be crucial in the control of neuronal plasticity both during development and after CNS injury – the formation of mature PNNs signals the closure of neuronal plasticity [22, 23]. PNN removal after spinal cord injury enhances plasticity, for example, by allowing de novo sprouting of axons and the formation of new synapses for the recovery of function [24, 25]. Thus, excessive HA accumulation in the ECM of muscle increases its viscoelasticity and the resistance to passive movement and may also increase the sensitivity of the muscles spindles and exacerbate spasticity. In addition, it may disrupt peripheral plasticity which may be crucial for recovery of movement and function.

Catabolism of Hyaluronan by Hyaluronidases

Hyaluronidases were first described by Duran-Reynals who observed that extracts of mammalian testis and other tissues contain a “spreading factor” which could facilitate the diffusion of dyes and antiviral vaccines injected subcutaneously [26, 27]. The term “hyaluronidase” was introduced by Karl Meyer in 1971 to denote that the enzymes degrade HA. Meyer classified hyaluronidases based on biochemical analysis and the end products generated into mammalian hyaluronidases, leech hyaluronidase, and microbial hyaluronidases [28]. The initial degradation of HA is accomplished by hyaluronidase, which cleaves the linkage between glucuronic acid and N-acetyl glucosamine and generates oligosaccharides of different chain lengths which are the substrates for two other exoglycosidases [29] (Fig. 13.3a).

The human genome contains six hyaluronidase-like genes which share about 40% of their identity with one another, suggesting that they evolved by gene duplication, although the expression of each gene has a unique tissue distribution. The

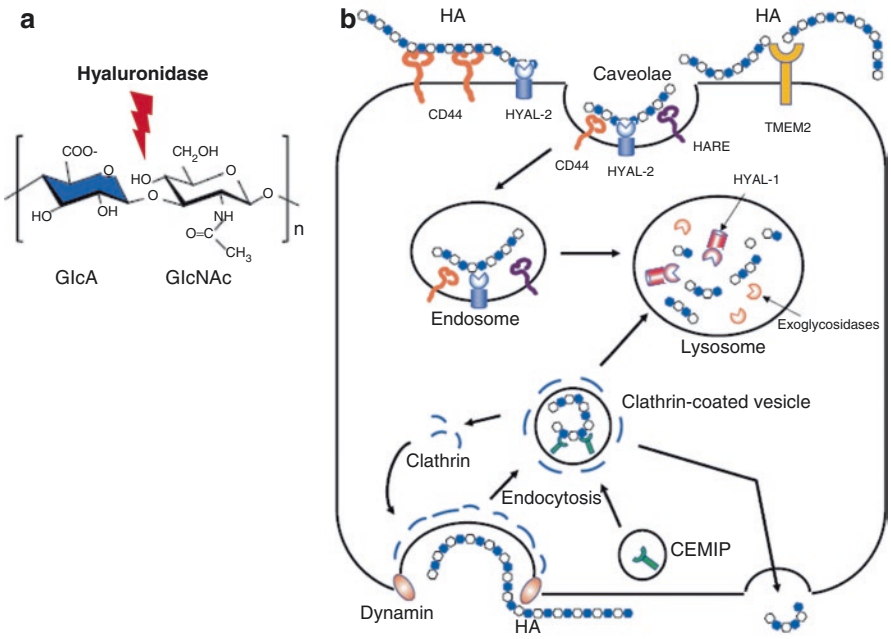

Fig. 13.3 Schematic illustration of mechanisms of hyaluronan (HA) degradation. (**a**) The initial degradation of HA is accomplished by hyaluronidase (HYAL), which cleaves the linkage between glucuronic acid and N-acetyl glucosamine and generates oligosaccharides of different chain lengths. (**b**) In HYAL-mediated HA degradation (top), high molecular weight HA is tethered to the cell surface by CD44 and GPI-anchored HYAL2 into caveolin-rich lipid rafts and then cleaved into approximately 2×10^4 Da fragments. The HA fragments are subsequently delivered to endo-lysosome compartments and degraded into smaller oligosaccharides by HYAL1 and monosaccharides by exoglycosidases. In the proposed model of CEMIP-mediated HA degradation (bottom), high-molecular-weight HA is endocytosed into clathrin-coated vesicles and cleaved into lower-molecular-weight HA fragments by the action of CEMIP, which is localized in the peripheral vesicles of the cell. The fragmented HA is then depolymerized in endo-lysosome compartments or released extracellularly without intracytoplasmic accumulation. TMEM2 is expressed on the cell surface in a type II transmembrane topology and degrades high molecular weight HA into approximately 5×10^3 Da fragments. (From Kobayashi T (2020), with permission)

genes HYAL1, HYAL2, and HYAL3 are located on chromosome 3p21.3, whereas HYAL4, PHYAL1 (a pseudogene), and sperm adhesion molecule 1 (SPAM1, also known as PH20) are clustered on chromosome 7p31.3. HYAL1 and HYAL2 are the major hyaluronidases expressed in human somatic tissues and are both needed for catabolism of tissue HA [30, 31]. HYAL1 plays an important role in HA degradation within the liver, whereas HYAL2 is required for clearance of high molecular weight HA in lymph nodes and plasma and for HA endocytosis by liver non-parenchymal cells [32].

In a recently proposed model of HA catabolism (Fig. 13.3b), the glycosylphosphatidylinositol (GPI)-anchored cell surface hyaluronidase HYAL2 cleaves high molecular weight HA into approximately 2×10^4 Da fragments at the cell surface

with the HA receptor CD44 [33]. The partially fragmented HA is internalized by binding to the HA receptors [34] and is then further degraded by HYAL1 and exoglycosidases in the lysosomal system. Interestingly, HYAL2 appears to favor an acidic pH for its hyaluronidase activities [35]. More recently, two novel molecules, the cell migration inducing protein (CEMIP/KIAA1199) and transmembrane protein 2 (TMEM2), have been identified that contribute to digesting extracellular high molecular weight HA into smaller fragments [36–38]. As the fragmented HA in the ECM is usually internalized by cells through receptors, HA receptors have roles not only in intracellular signaling but also in HA clearance [39–43].

Pharmacology and Uses of Exogenous Hyaluronidases

The interstitial connective tissue matrix is a complex three-dimensional dynamic structure comprised of numerous structural macromolecules including collagens, elastin, and fibronectin, in which GAGs such as HA and proteoglycans form a hydrated gel-like substance that allows the ECM to resist compressive forces. Collagens are the predominant fibers that hold tissues in place and maintain tissue integrity. HA acts as a barrier to bulk fluid flow through the interstitial collagenous matrix due to its hydration and viscosity [44]. While the concentration of HA is only 1% of the concentration of collagen in the skin, it occupies a fluid exclusion volume tenfold higher than that of collagen on a mL H_2O/mg basis [45]. In contrast to collagen, which has a half-life approaching 15 years [46], HA is rapidly turned over in the body with a half-life of 15–20 hours in the skin [47, 48]. Thus, HA in the skin and subcutaneous interstitial connective tissue matrix forms an effective dermal barrier.

"Spreading agents" derived from animal testes extracts containing interstitial matrix-degrading enzymes have been used clinically for over 50 years to facilitate the dispersion and absorption of other drugs through the skin and subcutaneous tissue, including procaine for patients with spasticity [28, 49]. SPAM1 or PH20 is the predominant hyaluronidase in mammalian testes and is the only neutral pH-active hyaluronidase that degrades GAGs under physiologic conditions. Thus, PH20 is used therapeutically to increase the speed of absorption of drugs, to promote resorption of excess fluids, to increase the effectiveness of local anesthesia, and to diminish tissue destruction by subcutaneous and intramuscular injection of fluids [50, 51]. While animal testes-derived hyaluronidase extracts have been used extensively in the clinic to disperse other injected drugs, they have generally been limited by both immunogenicity and impurity profiles, typically comprising less than 1% enzyme per mg total protein. Such preparations are frequently contaminated with proteases, immunoglobulin, and factors that increase capillary permeability and can also give rise to IgE-mediated allergic reactions upon repeat administration [52, 53].

The human PH20 enzyme is a 509 amino acid glycoprotein anchored to the plasma membrane through a GPI moiety that facilitates penetration of spermatozoa through the cumulus cells to enable fertilization [54]. A purified soluble recombinant human hyaluronidase (rHuPH20) lacking the GPI membrane attachment,

containing 447 amino acids with an approximate molecular weight of 61 kDa, is produced by genetically engineered Chinese hamster ovary (CHO) cells containing a DNA plasmid encoding for a soluble fragment of human hyaluronidase (PH20). Recombinant human hyaluronidase (Hylenex®, Halozyme Therapeutics, San Diego, California) enhances the infusion rates and penetration of molecules up to 200 nm in diameter up to 20-fold without eliciting inflammation, vascular permeability, and immunogenic or allergic reactions [55]. This product was FDA approved in 2005.

Recombinant human hyaluronidase is supplied as a sterile, clear, colorless, non-preserved, ready-for-use solution with an approximate pH of 7.0 and an osmolality of 280–340 mOsm/kg. It is indicated as an adjuvant in subcutaneous fluid administration for achieving hydration, to increase the dispersion and absorption of other injected drugs [56], and in subcutaneous urography for improving resorption of radiopaque agents. It is approved for infiltration use, interstitial use, intramuscular use, intraocular use, retrobulbar use, soft tissue use, and subcutaneous use. Hyaluronidase is antigenic; repeated injections of relatively large amounts of hyaluronidase preparations may result in the formation of neutralizing antibodies. However, allergic reactions have been reported in less than 0.1% of patients. Anaphylactic-like reactions following retrobulbar block or intravenous injections have occurred rarely. The most frequently reported adverse reactions have been mild local injection site reactions, such as erythema and pain. The long-term effects of hyaluronidase on fertility are unknown. It also has several off-label uses in dermatology, plastic surgery, ophthalmology, and surgery [56–61]. The use of hyaluronidase for the treatment of muscle stiffness is a novel off-label application at present.

Novel Off-Label Use of Hyaluronidase for Treatment of Muscle Stiffness

Upper Limb Muscle Stiffness

Safety and Preliminary Efficacy of a Single Injection Treatment

In an initial retrospective case series [1], 20 patients with unilateral upper limb spastic-muscle stiffness of cerebral origin received off-label injections of recombinant human hyaluronidase in combination with preservative-free normal saline into 6–8 upper limb muscles at a single visit. All patients (mean age 41 ± 22 years and mean time since injury 40.6 ± 38.9 months) had moderately severe unilateral upper limb spasticity across more than one joint, defined by a Modified Ashworth Scale (MAS) score ≥2. The dose ranged from 450 to 600 units of hyaluronidase diluted with normal saline which was distributed in multiple synergistically acting muscles.

There were no clinically significant adverse effects related to the treatment. Resistance to passive movement was assessed clinically using the MAS (see Chaps. 3 and 4). The percentage of joints with MAS = 3 decreased by 38.5% and those with MAS = 0 increased by 46.9% within 3 days to 2 weeks postinjection, suggesting a clear effect of the injections (Fig. 13.4). Passive range of motion

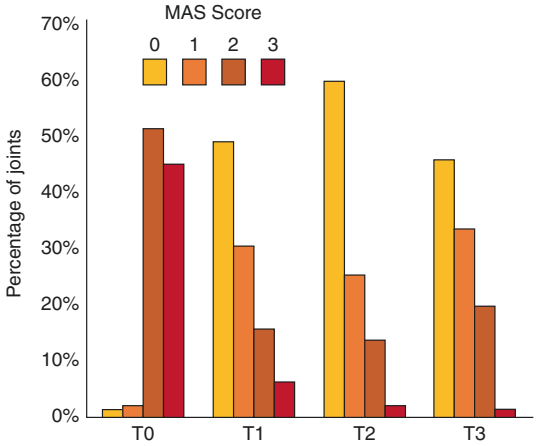

Fig. 13.4 Modified Ashworth Scale (MAS) score across upper limb joints at T0 = preinjection, T1 = within 2 weeks post hyaluronidase injection, T2 = within 4–6 weeks post hyaluronidase injection, and T3 = within 3–5 months post hyaluronidase injection. (Data from Raghavan P (2016), with permission)

(PROM) and active range of motion (AROM) were evaluated pre- and postinjection to assess clinical response to treatment. PROM at all joints and AROM at most joints increased within 2 weeks postinjection (T1) and persisted at 4–6 weeks postinjection (T2) and 3–5 months postinjection (T3) (Fig. 13.5). There was a delayed increase in active elbow extension and forearm pronation, which was unexpected, suggesting a possible effect on plasticity. The results persisted for at least 3 months. Most importantly, there were no side effects of muscle weakness or sedation. These results provide preliminary evidence that intramuscular hyaluronidase injections can reduce muscle stiffness and increase passive and active movement in multiple upper limb joints of patients with chronic muscle stiffness secondary to spasticity.

Safety and Dose-Response of Multiple Injection Treatments

In a follow-up retrospective study of 30 patients with moderate-to-severe muscle stiffness (approved by the New York University School of Medicine Institutional Review Board), the safety of multiple off-label hyaluronidase injections was assessed by examining the percentage of patients who had immediate or delayed hypersensitivity reactions or reported any adverse effects such as prolonged muscle soreness. The maximum total dose used in this cohort was 1575 IU, with a maximum of 300 IU injected into a single site at once, which is well below the threshold of toxicity of hyaluronidase [62]. Of the 30 subjects, 5 subjects had only one injection visit during the study period. The remaining subjects had multiple injection visits (range 2–10). The average time between injection visits was 17.7 weeks (range 4.2–57.5), and an average of 11.3 muscles (range 3.8–20.0) were injected per visit. The average volume injected per session was 14.1 ml (range 4.0–25.3), which equated to an average dose of 1054.4 units (range 300–1575) (unpublished data).

None of the subjects in this retrospective cohort demonstrated evidence of immediate hypersensitivity on intradermal testing, i.e., no erythema, itching, or wheal

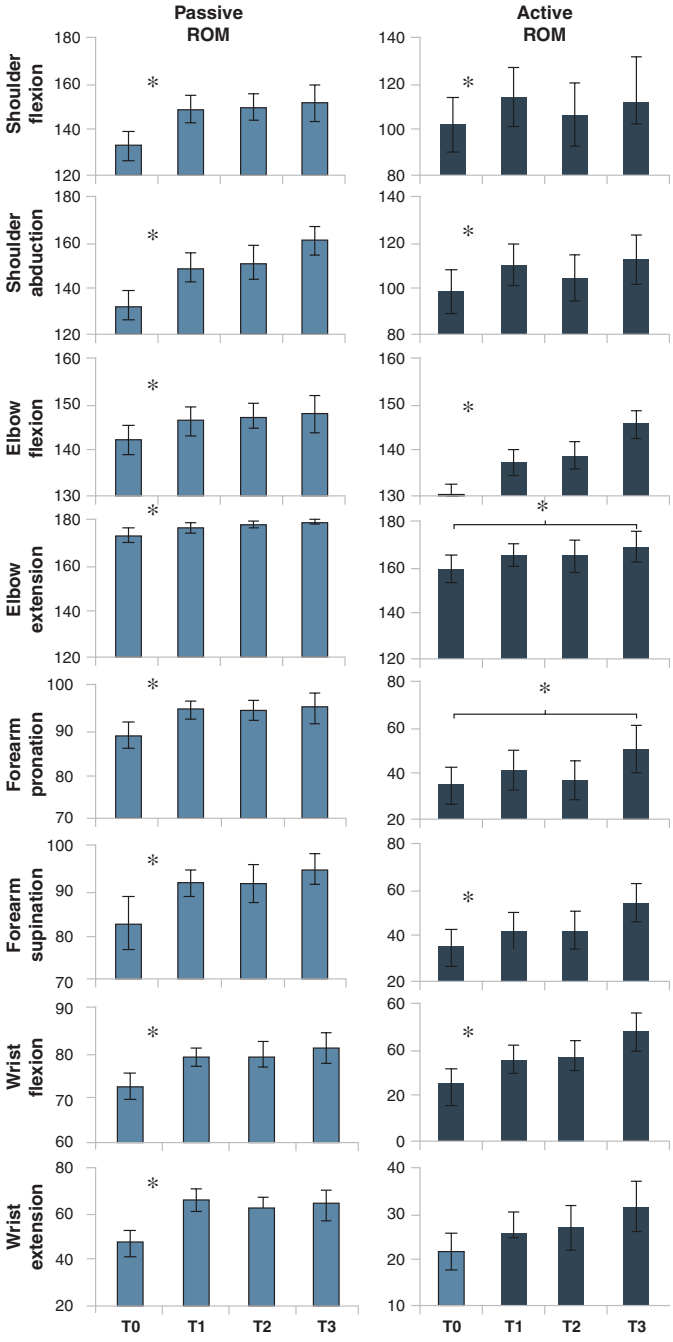

Fig. 13.5 Passive and active range of motion across upper limb joints (in degrees) at T0 = preinjection, T1 = within 2 weeks post hyaluronidase injection, T2 = within 4–6 weeks post hyaluronidase injection, and T3 = within 3–5 months post hyaluronidase injection. * statistically significant differences at $p < 0.05$. (Data from Raghavan P (2016), with permission)

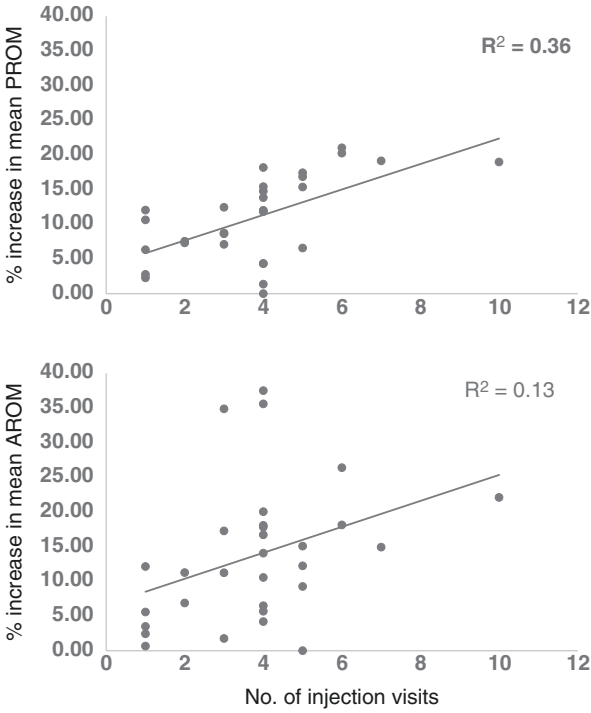

Fig. 13.6 Relationship between percentage change in average passive (PROM) and active range of motion (AROM) across the upper limb joints (shoulder abduction, shoulder flexion, elbow extension, elbow flexion, forearm supination, forearm pronation, wrist extension and wrist flexion) and the number of injection visits

was noted in or around the injection site prior to the intramuscular injections. None of them experienced delayed hypersensitivity. One subject had pain in the shoulder girdle which persisted after the injections and resolved once the statin that she was taking was discontinued. The subject continued to tolerate repeated injections without prolonged muscle soreness thereafter. No injection-related adverse effects were noted.

There was greater than 15% increase in maximum PROM from baseline in at least one joint in 87% (26/30) of subjects, and greater than 15% increase in maximum AROM from baseline in at least one joint in 70% (21/30) of subjects. As expected, ROM at baseline was negatively correlated with the percentage improvement in passive and active ROM, suggesting that the higher the baseline ROM, the less room for improvement. Across all joints, the improvements in PROM and AROM were correlated with the number of injection visits, suggesting an additive effect of repeat injections (Fig. 13.6). Subjects who showed little change in PROM showed changes in AROM and had lower levels of motor impairment at baseline, where as those who showed changes in PROM with little change in AROM had higher levels of motor impairment at baseline.

Lower Limb Muscle Stiffness

Preliminary Efficacy of a Single Injection Treatment

Off-label hyaluronidase has also been used clinically in the lower limb in several patients. Here, we present the changes in gait parameters in one patient who presented for instrumented gait analysis before and after the injections as part of an observational study (approved by the Johns Hopkins University Institutional Review Board). The patient, a 64-year-old woman, sustained left spastic hemiparesis and presented with muscle stiffness that affected her ability to walk. She was referred for off-label hyaluronidase injections by her neurologist to treat the muscle stiffness in her lower limbs. She underwent instrumented gait analysis prior to one set of injections and subsequently received 1500 units of human recombinant hyaluronidase distributed over 14 lower limb muscles, mostly on the left side at a single visit. Approximately two months postinjection, she underwent follow-up gait analysis. Note marked increases in the patient's gait speed (Table 13.1). Both her preferred and fastest comfortable walking speeds increased by nearly 20% (preferred, 1.05 m/s preinjection to 1.22 m/s postinjection; fastest comfortable, 1.20 m/s preinjection to 1.42 m/s postinjection). These improvements exceed reported minimal clinically important difference thresholds for persons with neurologic damage or disease. Instrumented gait analysis recorded lower extremity joint kinematics and ground reaction forces. The most noticeable changes in the patient's kinematics were observed in her left hip and knee, as extension in both joints improved by nearly 5 degrees following the injections (Fig. 13.7; note that the increased flexion in the right knee throughout the gait cycle was due to a previous orthopedic issue). These improvements in leg extension led to a 14% increase in the forward propulsion force generated by her left leg, which likely facilitated the observed increases

Table 13.1 Results of gait analysis pre- and postinjection

Gait parameters	Preinjection		Postinjection	
Ankle kinematics	Right	Left	Right	Left
Peak dorsiflexion (deg)	1.7	1.8	2.1	4.1
Peak plantarflexion (deg)	−31.6	−24.1	−31.8	−22.1
Knee kinematics				
Peak flexion (deg)	62.5	57.5	65.1	59.9
Peak extension (deg)	12.5	2.6	13.4	−2.7
Hip kinematics				
Peak flexion (deg)	25.3	23.6	27.9	25.8
Peak extension (deg)	−10.6	−17.0	−14.5	−21.8
Ground reaction forces				
Peak propulsion (N/kg)	0.17	0.14	0.19	0.16
Peak braking (N/kg)	−0.19	−0.15	−0.16	−0.24
Walking speeds				
Preferred (m/s)	1.05		1.22	
Fastest (m/s)	1.20		1.42	

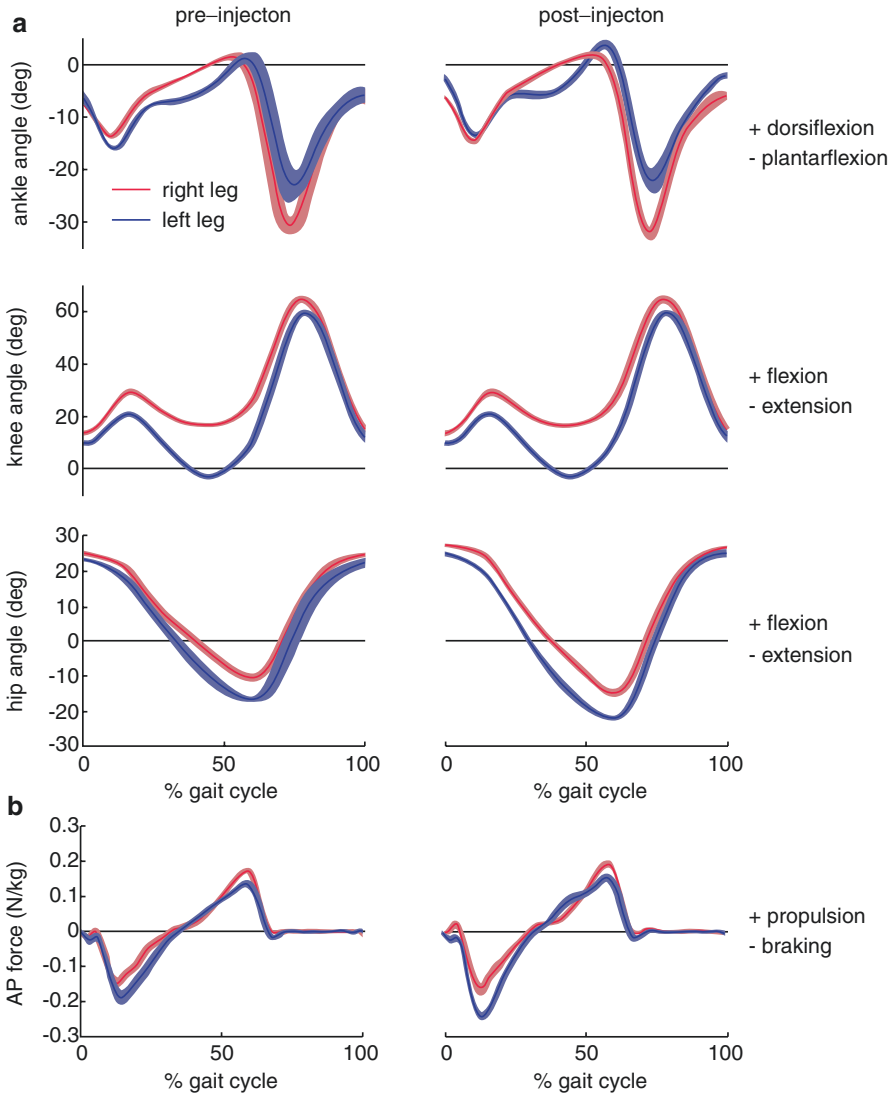

Fig. 13.7 Changes in gait parameters pre-post hyaluronidase injections to the lower limb muscles. (**a**) In joint kinematics. (**b**) In anteroposterior (AP) ground reaction forces

in gait speed. Importantly, these improvements were noticeable to the patient, as she perceived her gait to be smoother and more normal following the injections.

The clinical data presented above for the upper and lower limbs provides indirect evidence for the hyaluronan hypothesis, since HA content was not quantified. The results suggest that use of the enzyme hyaluronidase is a possible solution for the treatment of muscle stiffness associated with spasticity after neurological injury that does not cause muscle weakness [63, 64]. These results need to be confirmed in randomized controlled trials, one of which is currently ongoing (NCT03306615).

Imaging Quantification of Hyaluronan Content in Patients with Muscle Stiffness

T1rho (T1ρ) magnetic resonance imaging (MRI) mapping has been used to quantify GAG content in cartilage [65, 66], muscle [67–69], and intervertebral discs [70, 71]. T1ρ contrast is an endogenous noninvasive MRI contrast mechanism that refers to the spin lattice relaxation time constant in the rotating magnetic field and measures the transverse magnetization decay in the presence of a spin-lock radiofrequency (RF) field [72]. T1ρ contrast is sensitive to low energy interactions related to the chemical exchange between extracellular water and macromolecules and is well suited to characterize proteoglycan content [66, 73]. Hence, 3D-T1ρ MR mapping of the upper arm muscles was used to quantify intramuscular GAG content before and after hyaluronidase injection treatment [74]. Figure 13.8 shows representative mono-exponential T1ρ maps of the upper arm in controls and patients with post-stroke muscle stiffness before and after hyaluronidase injection treatment. Note the increased T1ρ relaxation times before the injections (middle panel, red) in the biceps and triceps muscles, reflecting increased intramuscular GAG content in patients with poststroke muscle stiffness. All three patients showed significant improvement in the T1ρ relaxation time of the biceps muscle within two weeks after treatment with hyaluronidase, approaching that of control values. The triceps muscle also showed increased GAG content but was not consistently targeted with the injections and therefore did not show a significant change given the small sample size. These results suggest that T1ρ mapping can be used to quantify GAG content in the muscles of patients with poststroke muscle stiffness noninvasively and that muscle HA content is increased in stiff muscles compared with controls, providing imaging corroboration for the hyaluronan hypothesis of muscle stiffness [74].

Accumulated Hyaluronan Traps Intramuscular Free Water in Stiff Muscles

In contrast to mono-exponential T1ρ mapping described above, bi-exponential T1ρ mapping can provide a more detailed characterization of the changes in the extracellular microenvironment (e.g., chemical exchange rate of protons, pH, GAG concentration, viscosity, and presence of free water) that contribute to the net increase observed in the mono-exponential T1ρ values shown in Fig. 13.8. The bi-exponential modeling uses a two-compartment model that breaks down the observed mono-exponential decay into its constituent parts, a short component that relaxes quickly and a long component that relaxes slowly. Increased GAG accumulation can increase the chemical exchange of the negatively charged GAGs with the protons of the water molecules, increasing the fraction of the short component. However, a more significant consequence is the aggregation of the GAGs into macromolecular spheres that trap free water in the ECM and increase the duration of the long component, T1ρl.

In patients with muscle stiffness, bi-exponential T1ρ mapping showed that the relaxation time of the short component was relatively unchanged, but the fraction of

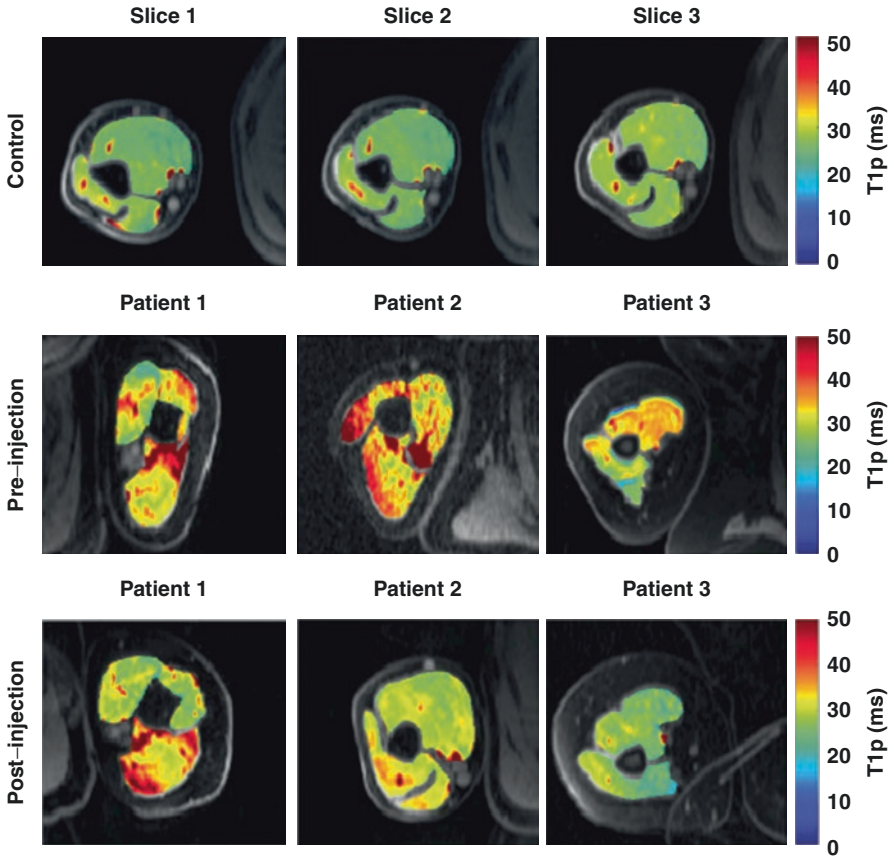

Fig. 13.8 Representative T1ρ maps of the upper arm in controls (top row) and patients with post-stroke muscle stiffness before (middle row) and after (bottom row) hyaluronidase injection treatment. Note the difference in relaxation times and the shape of the muscle before and after the injections. (From Menon R (2019), with permission)

the short component increased in the biceps and triceps muscles due to increased GAG accumulation (As (%)) (Table 13.2). In contrast, the relaxation time of the long component increased due to excessive free water in the ECM. Following treatment with hyaluronidase, note the shift of the mono-exponential and the bi-exponential short and long components with their corresponding fractions to values approaching those in controls. The changes in the fraction of the short component and the relaxation times of the long component provide an understanding of the role of intramuscular fluid accumulation in producing muscle stiffness. The results suggest that muscle stiffness is characterized by increased muscle GAG content and free water, both of which can be reduced with hyaluronidase injections. This pilot study demonstrates the application of bi-exponential T1rho mapping as a marker for GAG content in the muscle and as a potential treatment monitoring tool for patients with muscle stiffness [75].

Table 13.2 Summary of $T_{1\rho}$ mapping results

						P-values		
ROI	Fitting method	Parameter	Controls (n = 5)	Patients – pre (n = 5)	Patients – post (n = 3)	Patients vs. controls	Pre- vs. postinjection	Postinjection vs. controls
Biceps	Mono-exponential	Tlρm (ms)	26.7 ± 0.54	35.5 ± 2.93	29.45 ± 1.23	0.006	0.055	0.660
	Bi-exponential	Tlρs (ms)	7.12 ± 1.97	4.16 ± 3.25	7.72 ± 3.28	0.490	0.510	0.890
		Tlρl (ms)	37.32 ± 2.01	46.33 ± 5.57	48.14 ± 7.19	0.010	0.820	0.011
		As (%)	31.68 ± 8.54	52.21 ± 14.43	42.53 ± 9.17	0.031	0.410	0.070
		Al (%)	68.32 ± 8.54	47.79 ± 14.43	57.47 ± 9.17	0.031	0.410	0.070
Triceps	Mono-exponential	Tlρm (ms)	30.29 ± 2.23	34.57 ± 4.48	32.91 ± 4.9	0.138	0.730	0.500
	Bi-exponential	Tlρs (ms)	8.02 ± 3.26	6.06 ± 4.45	6.84 ± 1.40	0.930	0.90	0.460
		Tlρl (ms)	38.99 ± 4.89	50.5 ± 9.25	44.12 ± 6.13	0.004	0.280	0.150
		As (%)	28.06 ± 7.32	52.66 ± 20.29	42.54 ± 23.00	0.040	0.450	0.190
		Al (%)	71.94 ± 7.32	47.34 ± 20.29	57.46 ± 23.00	0.040	0.450	0.190

Mean T1rho values (± SD) for mono-exponential mean signal ($T_{1\rho m}$) and bi-exponential short signal and fraction ($T_{1\rho s}$, A_s) and long signal and fraction ($T_{1\rho l}$, A_l) in the biceps and triceps regions of interest (ROI) for controls and patients pre- and post hyaluronidase injection. (From Menon R (2021), with permission)

Patient and Muscle Selection for Treatment

The Preinjection Consultation

As for the use of any invasive treatment, including hyaluronidase injections, the preinjection evaluation visit should include a discussion with the patient about treatment goals, explanation of the treatment and procedure, and informed consent.

It must be clearly explained that treatment with hyaluronidase injections for muscle stiffness is off-label and is not yet approved by the FDA for this indication. The pros and cons of the injection of hyaluronidase versus other treatments, including the side effects such as the possibility of an allergic reaction and contingencies in case of one, should be explained. Other side effects can include temporary muscle soreness. The package insert may be provided along with literature on its off-label use for muscle stiffness.

A thorough explanation of the treatment must be provided by the clinician to the patient and family, regarding what it will entail, which muscles will be injected, the approximate number of injections, as well as the potential benefits and side effects. The pros include that it does not cause muscle weakness and that its effects can be additive with repeated treatments as shown in Fig. 13.6, although the incidence of tolerance is not known. The cons include the need for repeated treatments and that it cannot reverse fibrosis or contracture once these are established. Treatment goals must be discussed with the patient and family as suggested by the algorithm in Chap. 8.

Selection of Muscles

The selection of muscles for treatment depends on the goals of the treatment, the degree of stiffness, and the presence of fibrosis. Once these are determined, synergistically acting stiff muscles in one or more spatial planes along the myofascial chain may be selected for injection. Agonist and antagonist muscles across a joint must be treated in the same session for optimal effect [1]. The selection of muscles for injection and dosing requires specific training.

Clinical differentiation between muscle stiffness and contracture may be difficult in patients with severe muscle stiffness. This is important as there may be a critical window of opportunity in patients who are not yet contracted, as described in Chap. 6. Ultrasonography is a useful tool to visualize muscle tissue and infer its composition by assessing its echogenicity [76, 77]. Echo-intensity denotes the brightness of an image caused by the reflection of sound waves and is influenced by sound beam characteristics and tissue density [78]. Healthy muscles look dark with sharp bright lines on B-mode ultrasonography. The dark signal is hypoechoic, and the bright lines represent hyperechoic signal from collagen fibers in the endomysium and perimysium. Hyperechoic signal can be produced by fibrosis but also by fatty infiltration [79–81].

A qualitative assessment of muscle echo-intensity may be made using the grading described by the Heckmatt rating scale (Fig. 13.9a) [82]. The use of the Heckmatt rating scale has demonstrated that muscles showing high echo-intensity have a poorer response to treatment of spasticity with botulinum toxin injections [83–86]. On the other hand, trigger points (TrPs) are defined as stiff nodules in a taut band of muscle that present a hypoechoic signal [87, 88]. However, gray-scale ultrasonography cannot assess the mechanical properties of the muscle such as its stiffness, i.e., the ability of the muscle to be compressed, elongated, stretched, or manipulated.

Hence, shear wave elastography (SWE) has emerged as a quantitative measure of passive stiffness in individuals with spasticity and muscle stiffness, where an acoustic radiation force impulse or shear wave is generated by a special transducer and the local tissue deformation is evaluated using ultrasound imaging [89–92]. However, the use of SWE is limited by interobserver and technical variability, an inability to assess deeper muscles due to attenuation of the shear wave as it passes through the tissue, lack of standard protocols, and the need for specialized equipment [93–96].

The myotonometer is a handheld instrument which provides a mechanical impact to the muscle and measures the decaying oscillations that travel through it. The device can provide quantitative measurements of muscle properties such as tone, stiffness, and elasticity [97], which have been found to be reliable in assessing changes in muscle mechanical properties in individuals with spasticity [98–103]. The measurements of muscle properties with the myotonometer are highly correlated with those made using SWE [104], but they also suffer from similar drawbacks such as high interobserver and technical variability, inability to assess deeper muscles due to attenuation of the impulse as it passes through the tissue, lack of standard protocols, and the need for specialized equipment. Therefore, a more practical method in the clinical setting may be to qualitatively assess the compressibility of the underlying muscle by manual palpation to estimate the resistance of the tissue to displacement using the stiffness rating scale (Fig. 13.9b) [105].

The combined use of the qualitative assessment of muscle stiffness using the stiffness rating scale and of muscle echo-intensity using the Heckmatt rating scale is proposed to differentiate between severe muscle stiffness and contracture in the clinical setting. The stiffness-echogenicity matrix (SEM) combines echo-intensity using the Heckmatt rating scale on the x-axis with stiffness rating on the y-axis (Fig. 13.10). The combined echo-intensity and stiffness grades range from 1A (acutely denervated flaccid muscle) to 4D (noncompressible stiff and contracted muscle), representing a wide spectrum of conditions seen in clinical practice. It is proposed that muscles demonstrating high stiffness grades but low muscle echo-intensity on ultrasound, represented in the red box, are more likely to respond to treatment with hyaluronidase. Therefore, when there is a question about fibrosis or contracture, qualitative ultrasound may assist the clinician in decision-making.

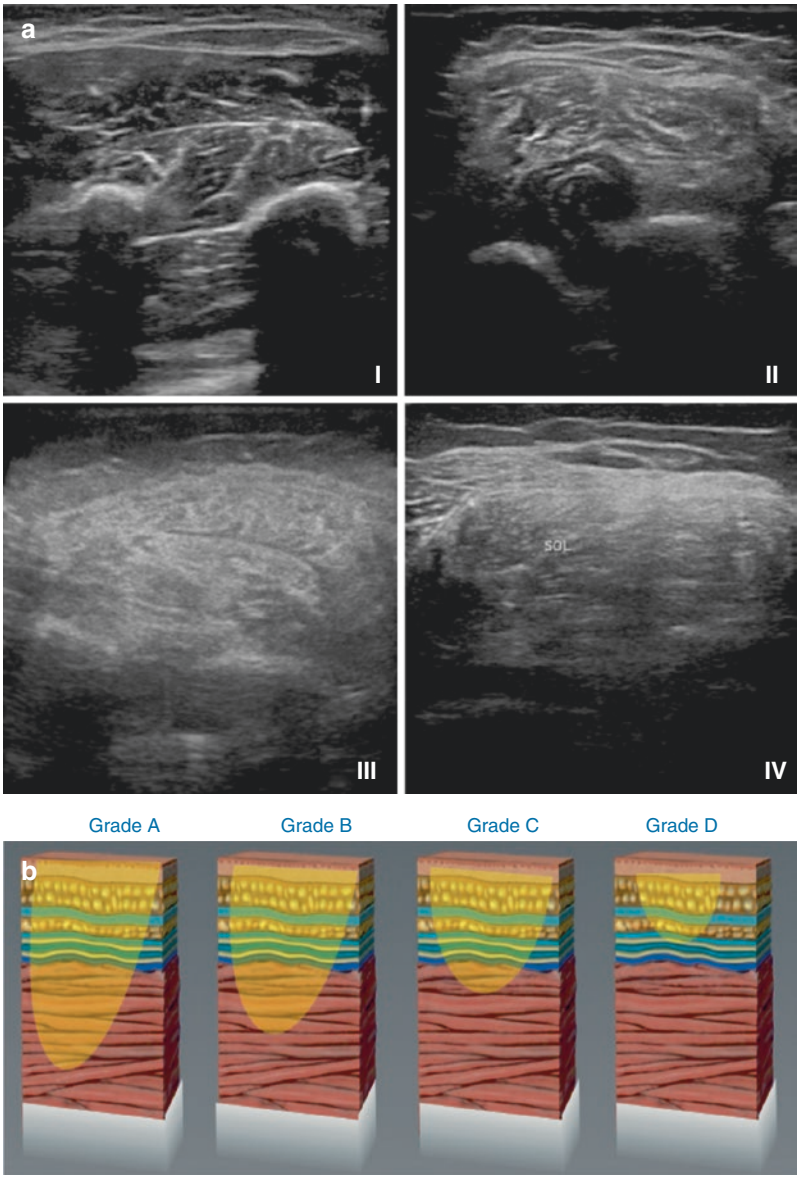

Fig. 13.9 Qualitative assessment of muscle stiffness and echogenicity. (**a**) Muscle echo can be graded by ultrasound using the Heckmatt rating scale, where the grades represent the following: I = Normal, II = Increase in echo intensity while bone echo is still distinct, III = Marked increase in muscle echo intensity with reduced bone echo, IV = Very high muscle echo intensity and complete loss of bone echo. (**b**) The stiffness rating scale assesses the compressibility of the underlying muscle by palpation to estimate the resistance of the tissue to displacement, where the grades represent the following: A = The muscle feels soft to the palpating thumb or index finger. It is possible to compress 75% of the relaxed muscle tissue, B = It is possible to compress only 50% of the relaxed muscle tissue due to mild resistance, C = It is possible to compress only 25% of the relaxed muscle tissue due to moderate resistance, D = It is impossible to compress the relaxed muscle tissue due to high resistance (bone-like). (From Stecco A (2019), with permission)

STIFFNESS–ECHOGENICITY MATRIX		ECHOGENICITY RATING			
		1	2	3	4
STIFFNESS RATING	A	1A Acute denervation	2A Atrophic muscle	3A Sacrcopenia	4A Severe Sacrcopenia
	B	1B Hypertrophic muscle	2B Normal	3B Early peripheral neurogenic	4B Early myogenic
	C	1C Densification	2C Chronic densification	3C Late peripheral neurogenic	4C Late myogenic
	D	1D Trigger points	2D Early central neurogenic	3D Central neurogenic	4D Late central neurogenic

Fig. 13.10 The Stiffness Echogenicity Matrix (SEM) combines qualitative rating of muscle stiffness using the stiffness rating scale on the y-axis with rating of muscle echo-intensity using the Heckmatt rating scale on the x-axis. The cells in the SEM represent a wide spectrum of conditions seen in clinical practice. The color of each cell in the matrix reflects the echo-intensity on gray-scale ultrasound. The red box highlights muscles with high stiffness but low echo that may respond to treatment with hyaluronidase. (From Stecco A (2019), with permission)

The Injection

In previous studies, we diluted the commercially available hyaluronidase so as to optimize the volume and pressure of the injection [106]. Dilution also resulted in a lower dosage overall across all the muscles injected as the goal is to inject just enough enzyme to catabolize excessive HA in the stiff muscles. The dilution and dosage for individual muscles may vary based on the degree of muscle stiffness and the underlying disease and requires additional study. As with any invasive procedure, aseptic technique must be used, and precautions must be taken to avoid intravascular injection.

Hyaluronidase injections do not target the motor end plate; hence, the use of electromyography or electrical stimulation guidance is not necessary. However, ultrasound guidance may be helpful to confirm the anatomy in regions where surface anatomy is not clear or where there are critical neurovascular structures.

After Injection

Patients should be advised to use a warm compress for local soreness around the injection sites. Given that immobility can contribute to the accumulation and biophysical alteration of HA, patients should be encouraged to perform passive, active-passive (bimanually assisted), and/or active movements and stretching exercises to restore muscle length. Therapy to retrain functional movements and prevent compensatory muscle use may also be necessary. It is helpful to assess the patient 2–4 weeks after the injections to determine the effect of treatment and dosing and muscle selection for future injections.

Measuring Outcomes

Standardized measures before and after treatment are integral components of the assessment process. The most proximate outcome of the treatment of muscle stiffness with hyaluronidase is a change in passive range of motion at multiple joints in the limb, which may depend on the muscles selected for treatment, the degree of stiffness, and the presence of fibrosis, as well as on baseline movement ability. Functional outcomes are important to patients, and must also be assessed, although these may take time to change. Reduction in discomfort, pain, and the ability to participate in daily life roles are also important to assess.

Conclusions

Although spasticity develops because of injury to the CNS, peripheral non-neural mechanisms contribute to the ensuing muscle stiffness. The hyaluronan hypothesis postulates that the accumulation and biophysical alteration of hyaluronan within the ECM of muscle can lead to muscle stiffness. The use of hyaluronidase has emerged as a potential treatment to catabolize the excessive hyaluronan, which if left untreated may contribute to progression to muscle fibrosis and contracture. Randomized controlled clinical trials are needed to confirm preliminary findings of the efficacy of hyaluronidase in the treatment of muscle stiffness and in the prevention of fibrosis and muscle contracture. A better understanding of the mechanisms underlying muscle stiffness, the basis for treatment with hyaluronidase, and the dosing parameters, can potentially transform clinical practice for the treatment of muscle stiffness in both spastic and non-spastic patient populations.

Disclosures This chapter discusses the off-label use of hyaluronidase for treatment of muscle stiffness. Drs. Preeti Raghavan and Antonio Stecco are co-founders of MovEase, Inc.

References

1. Raghavan P, et al. Human recombinant hyaluronidase injections for upper limb muscle stiffness in individuals with cerebral injury: a case series. EBioMedicine. 2016;9:306–13.
2. Stecco A, Stecco C, Raghavan P. Peripheral mechanisms of spasticity and treatment implications. Curr Phys Med Rehabil Rep. 2014;2(2):121–7.
3. Piehl-Aulin K, et al. Hyaluronan in human skeletal muscle of lower extremity: concentration, distribution, and effect of exercise. J Appl Physiol (1985). 1991;71(6):2493–8.
4. Purslow PP, Trotter JA. The morphology and mechanical properties of endomysium in series-fibred muscles: variations with muscle length. J Muscle Res Cell Motil. 1994;15(3):299–308.
5. Cowman MK, et al. Viscoelastic properties of hyaluronan in physiological conditions. F1000Res. 2015;4:622.
6. Okita M, et al. Effects of reduced joint mobility on sarcomere length, collagen fibril arrangement in the endomysium, and hyaluronan in rat soleus muscle. J Muscle Res Cell Motil. 2004;25(2):159–66.

7. Calve S, et al. Hyaluronic acid, HAS1, and HAS2 are significantly upregulated during muscle hypertrophy. Am J Physiol Cell Physiol. 2012;303(5):C577–88.
8. Menon RG, et al. T1rho-mapping for musculoskeletal pain diagnosis: case series of variation of water bound glycosaminoglycans quantification before and after fascial manipulation((R)) in subjects with elbow pain. Int J Environ Res Public Health. 2020;17(3).
9. Meyer GA, McCulloch AD, Lieber RL. A nonlinear model of passive muscle viscosity. J Biomech Eng. 2011;133(9):091007.
10. Elliott DM, et al. Effect of altered matrix proteins on quasilinear viscoelastic properties in transgenic mouse tail tendons. Ann Biomed Eng. 2003;31(5):599–605.
11. Richter RP, et al. Glycosaminoglycans in extracellular matrix organisation: are concepts from soft matter physics key to understanding the formation of perineuronal nets? Curr Opin Struct Biol. 2018;50:65–74.
12. Gibbs DA, et al. Rheology of hyaluronic acid. Biopolymers. 1968;6(6):777–91.
13. Matteini P, et al. Structural behavior of highly concentrated hyaluronan. Biomacromolecules. 2009;10(6):1516–22.
14. Geiringer SR, deLateur BJ. Physiatric therapeutics. 3. Traction, manipulation, and massage. Arch Phys Med Rehabil. 1990;71(4-S):S264–6.
15. deLateur BJ, Hinderer SR. Physiatric therapeutics. 2. Therapeutic heat and cold, electrotherapy, and therapeutic exercise. Arch Phys Med Rehabil. 1990;71(4-S):S260–3.
16. Li S, et al. Different effects of cold stimulation on reflex and non-reflex components of post-stroke spastic hypertonia. Front Neurol. 2017;8:169.
17. Magnusson SP. Passive properties of human skeletal muscle during stretch maneuvers. A review. Scand J Med Sci Sports. 1998;8(2):65–77.
18. Gao F, et al. Effects of repeated ankle stretching on calf muscle-tendon and ankle biomechanical properties in stroke survivors. Clin Biomech (Bristol, Avon). 2011;26(5):516–22.
19. Stecco C, et al. Hyaluronan within fascia in the etiology of myofascial pain. Surg Radiol Anat. 2011;33(10):891–6.
20. Margalef R, et al. Experimental myofascial trigger point creation in rodents. J Appl Physiol (1985). 2019;126(1):160–9.
21. Fukami Y. Studies of capsule and capsular space of cat muscle spindles. J Physiol. 1986;376:281–97.
22. Kwok JC, Carulli D, Fawcett JW. In vitro modeling of perineuronal nets: hyaluronan synthase and link protein are necessary for their formation and integrity. J Neurochem. 2010;114(5):1447–59.
23. Kwok JC, et al. Extracellular matrix and perineuronal nets in CNS repair. Dev Neurobiol. 2011;71(11):1073–89.
24. Smith PD, et al. "GAG-ing with the neuron": the role of glycosaminoglycan patterning in the central nervous system. Exp Neurol. 2015;274(Pt B):100–14.
25. Carulli D, Kwok JC, Pizzorusso T. Perineuronal nets and CNS plasticity and repair. Neural Plast. 2016;2016:4327082.
26. Duran-Reynals F. Exaltation de l'activité du virus vaccinal par les extraits de certains organs. Comptes Rendus des Séances de la Société de Biologie et de Ses Filiales. 1928;99:6–7.
27. Chain E, Duthie ES. Identity of hyaluronidase and spreading factor. Br J Exp Pathol. 1940;21:324–38.
28. Meyer K. Hyaluronidases. In: Boyer PD, editor. The enzymes. New York: Academic Press; 1971. p. 307–20.
29. Roden L, et al. Enzymic pathways of hyaluronan catabolism. Ciba Found Symp. 1989;143:60–76; discussion 76–86, 281–5.
30. Csoka AB, Frost GI, Stern R. The six hyaluronidase-like genes in the human and mouse genomes. Matrix Biol. 2001;20(8):499–508.
31. Stern R. Devising a pathway for hyaluronan catabolism: are we there yet? Glycobiology. 2003;13(12):105R–15R.
32. Bourguignon V, Flamion B. Respective roles of hyaluronidases 1 and 2 in endogenous hyaluronan turnover. FASEB J. 2016;30(6):2108–14.

33. Kobayashi T, Chanmee T, Itano N. Hyaluronan: metabolism and function. Biomolecules. 2020;10(11).
34. Culty M, Nguyen HA, Underhill CB. The hyaluronan receptor (CD44) participates in the uptake and degradation of hyaluronan. J Cell Biol. 1992;116(4):1055–62.
35. Afify AM, et al. Purification and characterization of human serum hyaluronidase. Arch Biochem Biophys. 1993;305(2):434–41.
36. Yoshida H, et al. KIAA1199, a deafness gene of unknown function, is a new hyaluronan binding protein involved in hyaluronan depolymerization. Proc Natl Acad Sci U S A. 2013;110(14):5612–7.
37. Yamamoto H, et al. A mammalian homolog of the zebrafish transmembrane protein 2 (TMEM2) is the long-sought-after cell-surface hyaluronidase. J Biol Chem. 2017;292(18):7304–13.
38. Yamaguchi Y, et al. TMEM2: a missing link in hyaluronan catabolism identified? Matrix Biol. 2019;78-79:139–46.
39. McGary CT, et al. Degradation and intracellular accumulation of a residualizing hyaluronan derivative by liver endothelial cells. Hepatology. 1993;18(6):1465–76.
40. McGary CT, Raja RH, Weigel PH. Endocytosis of hyaluronic acid by rat liver endothelial cells. Evidence for receptor recycling. Biochem J. 1989;257(3):875–84.
41. Zhou B, et al. Purification and subunit characterization of the rat liver endocytic hyaluronan receptor. J Biol Chem. 1999;274(48):33831–4.
42. Fraser JR, Appelgren LE, Laurent TC. Tissue uptake of circulating hyaluronic acid. A whole body autoradiographic study. Cell Tissue Res. 1983;233(2):285–93.
43. Fraser JR, et al. Plasma clearance, tissue distribution and metabolism of hyaluronic acid injected intravenously in the rabbit. Biochem J. 1981;200(2):415–24.
44. Day TD. The permeability of interstitial connective tissue and the nature of the interfibrillary substance. J Physiol. 1952;117(1):1–8.
45. Craig AS, Eikenberry EF, Parry DA. Ultrastructural organization of skin: classification on the basis of mechanical role. Connect Tissue Res. 1987;16(3):213–23.
46. Verzijl N, et al. Effect of collagen turnover on the accumulation of advanced glycation end products. J Biol Chem. 2000;275(50):39027–31.
47. Laurent UB, Dahl LB, Reed RK. Catabolism of hyaluronan in rabbit skin takes place locally, in lymph nodes and liver. Exp Physiol. 1991;76(5):695–703.
48. Fraser JR, Laurent TC. Turnover and metabolism of hyaluronan. Ciba Found Symp. 1989;143:41–53; discussion 53–9, 281–5.
49. Locke RK. Treatment of spastic flatfoot with procaine-hyaluronidase and stretching. J Natl Assoc Chirop. 1952;42(11):36–8.
50. Frost GI, Csoka T, Stern R. The hyaluronidases: a chemical, biological and clinical overview. Trends Glycosci Glycotechnol. 1996;8:419–34.
51. Farr C, et al. Clinical pharmacology and possible applications of hyaluronidase with reference to Hylase "Dessau". Wien Med Wochenschr. 1997;147(15):347–55.
52. Eberhart AH, Weiler CR, Erie JC. Angioedema related to the use of hyaluronidase in cataract surgery. Am J Ophthalmol. 2004;138(1):142–3.
53. Williams RG. The effects of continuous local injection of hyaluronidase on skin and subcutaneous tissue in rats. Anat Rec. 1955;122(3):349–61.
54. Lin Y, et al. A hyaluronidase activity of the sperm plasma membrane protein PH-20 enables sperm to penetrate the cumulus cell layer surrounding the egg. J Cell Biol. 1994;125(5):1157–63.
55. Bookbinder LH, et al. A recombinant human enzyme for enhanced interstitial transport of therapeutics. J Control Release. 2006;114(2):230–41.
56. Kang DW, et al. Recombinant human hyaluronidase PH20 (rHuPH20) facilitates subcutaneous infusions of large volumes of immunoglobulin in a swine model. Drug Deliv Transl Res. 2012;2(4):254–64.
57. Sharma DSC, Lahiri MA. Use of hyaluronidase in plastic surgery: a review. J Plast Reconstr Aesthet Surg. 2021;74(7):1610–4.

58. Searle T, Ali FR, Al-Niaimi F. Hyaluronidase in dermatology: uses beyond hyaluronic acid fillers. J Drugs Dermatol. 2020;19(10):993–8.
59. Helm Ii S, Racz G. Hyaluronidase in neuroplasty: a review. Pain Physician. 2019;22(6):555–60.
60. Dunn AL, et al. Hyaluronidase: a review of approved formulations, indications and off-label use in chronic pain management. Expert Opin Biol Ther. 2010;10(1):127–31.
61. Bailey SH, Fagien S, Rohrich RJ. Changing role of hyaluronidase in plastic surgery. Plast Reconstr Surg. 2014;133(2):127e–32e.
62. Seifter J. Studies on the pharmacology and toxicology of testicular hyaluronidase. Ann N Y Acad Sci. 1950;52(7):1141–55.
63. Mayer NH. New treatment approaches on the horizon for spastic hemiparesis. PM R. 2018;10(9 Suppl 2):S144–50.
64. Raghavan P. Emerging therapies for spastic movement disorders. Phys Med Rehabil Clin N Am. 2018;29(3):633–44.
65. Keenan KE, et al. Prediction of glycosaminoglycan content in human cartilage by age, T1rho and T2 MRI. Osteoarthr Cartil. 2011;19(2):171–9.
66. Mlynarik V, et al. Transverse relaxation mechanisms in articular cartilage. J Magn Reson. 2004;169(2):300–7.
67. Wang L, Regatte RR. T(1)rho MRI of human musculoskeletal system. J Magn Reson Imaging. 2015;41(3):586–600.
68. Sharafi A, Chang G, Regatte RR. Bi-component T1rho and T2 relaxation mapping of skeletal muscle in-vivo. Sci Rep. 2017;7(1):14115.
69. Peng XG, et al. Noninvasive assessment of age, gender, and exercise effects on skeletal muscle: initial experience with T1 rho MRI of calf muscle. J Magn Reson Imaging. 2017;46(1):61–70.
70. Paul CPL, et al. Quantitative MRI in early intervertebral disc degeneration: T1rho correlates better than T2 and ADC with biomechanics, histology and matrix content. PLoS One. 2018;13(1):e0191442.
71. Samartzis D, et al. Novel diagnostic and prognostic methods for disc degeneration and low back pain. Spine J. 2015;15(9):1919–32.
72. Sepponen RE, et al. A method for T1 rho imaging. J Comput Assist Tomogr. 1985;9(6):1007–11.
73. Gilani IA, Sepponen R. Quantitative rotating frame relaxometry methods in MRI. NMR Biomed. 2016;29(6):841–61.
74. Menon RG, Raghavan P, Regatte RR. Quantifying muscle glycosaminoglycan levels in patients with post-stroke muscle stiffness using T1rho MRI. Sci Rep. 2019;9(1):14513.
75. Menon RG, Raghavan P, Regatte RR. Pilot study quantifying muscle glycosaminoglycan using bi-exponential T1rho mapping in patients with muscle stiffness after stroke. Sci Rep. 2021;11(1):13951.
76. Pillen S, van Alfen N. Skeletal muscle ultrasound. Neurol Res. 2011;33(10):1016–24.
77. Correa-de-Araujo R, et al. The need for standardized assessment of muscle quality in skeletal muscle function deficit and other aging-related muscle dysfunctions: a symposium report. Front Physiol. 2017;8:87.
78. Iftekharuddin KM, Awwal AAS. Field guide to image processing. SPIE field guides. Bellingham, WA: SPIE Press; 2012.
79. Pillen S, et al. Skeletal muscle ultrasound: correlation between fibrous tissue and echo intensity. Ultrasound Med Biol. 2009;35(3):443–6.
80. Nijboer-Oosterveld J, Van Alfen N, Pillen S. New normal values for quantitative muscle ultrasound: obesity increases muscle echo intensity. Muscle Nerve. 2011;43(1):142–3.
81. Reimers K, et al. Skeletal muscle sonography: a correlative study of echogenicity and morphology. J Ultrasound Med. 1993;12(2):73–7.
82. Heckmatt JZ, Leeman S, Dubowitz V. Ultrasound imaging in the diagnosis of muscle disease. J Pediatr. 1982;101(5):656–60.
83. Kenis-Coskun O, et al. Reliability of quantitative ultrasound measurement of flexor digitorum superficialis and profundus muscles in stroke. J Comp Eff Res. 2020;9(18):1293–300.

84. Picelli A, et al. Ultrasonographic evaluation of botulinum toxin injection site for the medial approach to tibialis posterior muscle in chronic stroke patients with spastic equinovarus foot: an observational study. Toxins (Basel). 2017;9(11).
85. Hara T, et al. Effects of botulinum toxin A therapy and multidisciplinary rehabilitation on lower limb spasticity classified by spastic muscle echo intensity in post-stroke patients. Int J Neurosci. 2018;128(5):412–20.
86. Picelli A, et al. Is spastic muscle echo intensity related to the response to botulinum toxin type A in patients with stroke? A cohort study. Arch Phys Med Rehabil. 2012;93(7):1253–8.
87. Sikdar S, et al. Assessment of myofascial trigger points (MTrPs): a new application of ultrasound imaging and vibration sonoelastography. Annu Int Conf IEEE Eng Med Biol Soc. 2008;2008:5585–8.
88. Ozcakar L, et al. Ultrasound imaging for sarcopenia, spasticity and painful muscle syndromes. Curr Opin Support Palliat Care. 2018;12(3):373–81.
89. Brandenburg JE, et al. Quantifying passive muscle stiffness in children with and without cerebral palsy using ultrasound shear wave elastography. Dev Med Child Neurol. 2016;58(12):1288–94.
90. Jakubowski KL, et al. Passive material properties of stroke-impaired plantarflexor and dorsiflexor muscles. Clin Biomech (Bristol, Avon). 2017;49:48–55.
91. Brandenburg JE, et al. Quantifying effect of onabotulinum toxin a on passive muscle stiffness in children with cerebral palsy using ultrasound shear wave elastography. Am J Phys Med Rehabil. 2018;97(7):500–6.
92. Vigotsky AD, Rouse EJ, Lee SSM. Mapping the relationships between joint stiffness, modeled muscle stiffness, and shear wave velocity. J Appl Physiol (1985). 2020;129(3):483–91.
93. Boulard C, Gautheron V, Lapole T. Mechanical properties of ankle joint and gastrocnemius muscle in spastic children with unilateral cerebral palsy measured with shear wave elastography. J Biomech. 2021;124:110502.
94. Zuniga LDO, Lopez CAG, Gonzalez ER. Ultrasound elastography in the assessment of the stiffness of spastic muscles: a systematic review. Ultrasound Med Biol. 2021;47(6):1448–64.
95. Tran A, Gao J. Quantitative ultrasound to assess skeletal muscles in post stroke spasticity. J Cent Nerv Syst Dis. 2021;13:1179573521996141.
96. Lehoux MC, et al. Shear wave elastography potential to characterize spastic muscles in stroke survivors: literature review. Clin Biomech (Bristol, Avon). 2020;72:84–93.
97. Leonard CT, et al. Myotonometer intra- and interrater reliabilities. Arch Phys Med Rehabil. 2003;84(6):928–32.
98. Chuang LL, et al. Quantitative mechanical properties of the relaxed biceps and triceps brachii muscles in patients with subacute stroke: a reliability study of the myoton-3 myometer. Stroke Res Treat. 2012;2012:617694.
99. Li X, et al. Assessing muscle compliance in stroke with the Myotonometer. Clin Biomech (Bristol, Avon). 2017;50:110–3.
100. Chuang LL, Wu CY, Lin KC. Reliability, validity, and responsiveness of myotonometric measurement of muscle tone, elasticity, and stiffness in patients with stroke. Arch Phys Med Rehabil. 2012;93(3):532–40.
101. Chuang LL, et al. Relative and absolute reliabilities of the myotonometric measurements of hemiparetic arms in patients with stroke. Arch Phys Med Rehabil. 2013;94(3):459–66.
102. Aarrestad DD, et al. Intra- and interrater reliabilities of the Myotonometer when assessing the spastic condition of children with cerebral palsy. J Child Neurol. 2004;19(11):894–901.
103. Rydahl SJ, Brouwer BJ. Ankle stiffness and tissue compliance in stroke survivors: a validation of Myotonometer measurements. Arch Phys Med Rehabil. 2004;85(10):1631–7.
104. Lee Y, Kim M, Lee H. The measurement of stiffness for major muscles with shear wave elastography and myoton: a quantitative analysis study. Diagnostics (Basel). 2021;11(3).
105. Stecco A, et al. Stiffness and echogenicity: development of a stiffness-echogenicity matrix for clinical problem solving. Eur J Transl Myol. 2019;29(3):8476.
106. Hechter O. Studies on spreading factors: I. The importance of mechanical factors in hyaluronidase action in skin. J Exp Med. 1947;85(1):77–97.